International Journal of Research and Innovations in Earth Science
Volume 5, Issue 6, ISSN (Online): 2394-1375

Parameterization of Drop Size Distribution with Rainfall Rate: Comparison of the N(D) and R(D) Functions; and Relationship between Gamma and Lognormal Laws

Sounmaïla Moumouni [(1)*], Loic Saturnin Adjikpe [(2)], Siaka Massou [(2)] and Agnide Emmanuel Lawin [(3)]
[(1)] Higher Teachers' Training School of Natitingou, University of Parakou, Benin.
[(2)] Faculty of Sciences and Technology, University of Abomey-Calavi, Benin.
[(3)] National Water Institute, University of Abomey-Calavi, Benin.

Abstract **– The Drop Size Distributions (DSDs) measured in northern Benin (West Africa) are analyzed with $N(D)$ and $R(D)$ functions. The $N(D)$ function represents the number of raindrops per unit of volume and by interval of diameters, while the $R(D)$ function represents the rainfall rate per range of diameters. Meteorological variables that are formulated with the $N(D)$ function can also be formulated with the $R(D)$ function. In addition, the $R(D)$ function has the advantage of being independent of the falling drop speed which is not measured well enough by the disdrometers. In this paper, the averages of DSDs per rainfall class are modeled by the gamma and lognormal laws. The parameters of these models are adjusted according to the rain rate. We thus obtained DSD parameterized with the rate of rain. Evaluating the efficiency of this parameterization, we noticed that the $R(D)$ function estimates its useful moments better than the $N(D)$ function. Moreover, we have noted that DSD modeling by the gamma law is not significantly different from DSD modeling by the lognormal law. Furthermore, we have established a relation between the shape parameters of these two laws: $ln^2\sigma = ln\left(\frac{\mu+2}{\mu+1}\right), \forall\, \mu \in]-1, +\infty[$.**

Keywords **– Drop Size Distributions (DSD), Gamma and Lognormal Laws, Optical Disdrometer, Rainfall Rate.**

I. Introduction

Most works ([1]-[12]; etc.) which followed that of [13] on the Drop Size Distribution (DSD) analyze it using a generalized function $N(D)$. It is defined by spectrum of a given period T (one minute). It corresponds to the number of raindrops per unit of volume and by interval of diameters and is calculated as follows:

$$N(D_i) = \frac{N_i}{ST\Delta D_i Vt(D_i)} \qquad (1)$$

D_i is the equivalent diameter of the raindrops measured. ΔD_i is the width of the range of diameter centered on D_i. In this study, D_i and ΔD_i are expressed in millimeters. S is the disdrometer collecting surface area expressed in square meter. At the period T, N_i is the number of drops counted by the disdrometer in each size range. $V(D_i)$ is the falling speed of the drops of diameter D_i. For the rain rate to be proportional to a moment of $N(D)$ function, the relationship between the speed of falling drops and its diameter is used as suggested by [14] :

$$V(D_i) = 3.78 D_i^{0.67} [m \cdot s^{-1}] \qquad (2)$$

In our study, T is 60 seconds. Therefore, $N(D_i)$ is expressed in $[m^{-3} mm^{-1}]$.

Recently, [15] proposed a new function $R(D)$ to analyze the DSD. This function has the advantage of being independent of the falling speed of the drops. It is equal to the rainfall rate per diameter class. It is defined by the following expression:

$$R(D_i) = \frac{6\pi 10^{-4} N_i D_i^3}{ST\Delta D_i} \qquad (3)$$

These authors modeled the DSD using this function and showed that the model obtained, estimates well the radar reflectivity (in the approximation of Rayleigh) from the rain rate. We present in Table 1.a and 1.b some meteorological variables derived from the DSD using the $N(D)$ function or the $R(D)$ function.

In the West African region, the first studies on Drops Size Distribution (DSD) have been conducted by [16] and have been pursued by both [17] and [18]. These distributions had been observed with the impact disdrometer in Abidjan, Boyélé, Dakar and Niamey (Fig. 1). [19] Described the global characteristics of DSDs in West Africa compared with those of other climatic regions. This work highlighted a remarkable difference between the shape of DSDs of the temperate regions and that of the tropical regions. These authors also analyzed the variability of DSD within the West African region. They noticed that the moderate rain rates (2 to 20 mm/h) are generated by a large number of raindrops on the coastal sites, whereas on continental sites, a low number of raindrops is enough to produce the same rain rates. Furthermore, the DSDs observed in Niamey (Sahelian zone) are clearly distinguished from those observed in wet tropical zone (Abidjan and Boyele) based on relatively higher average size of their drops. Recently, [12] analyzed the DSD collected with optical disdrometers in the same region. They showed that these spectra have a marked convex shape, characteristic of a relative deficit in small drops, as already observed in the region by the previous authors. They also indicated that this form of DSD is well reproduced by the gamma law with three parameters and proved that these DSD are very deficient in raindrops number compared to rains of temperate regions.

The objective of this article is to parameterize DSDs measured in northern Benin with the rainfall rate. Specifically, we will: model the average DSDs by class of rainfall rate, using the $N(D)$ and $R(D)$ functions; adjust the model parameters according to the rainfall rate; and

International Journal of Research and Innovations in Earth Science
Volume 5, Issue 6, ISSN (Online): 2394-1375

compare the modeling of the DSD by the gamma law with the modeling of the DSD by the lognormal law.

Table 1.a. Expressions of meteorological variables formulated with the DSD using $N(D)$ function (more details in [15]).

Name of variables (Order of M_n)	Formula
The measured moment of the DSD (n)	$M_n = \sum_i D_i^n N(D_i)\Delta D_i \quad (4.a)$
The theoretical moment of the DSD (n)	$M_n = \int_0^{+\infty} D^n N(D) dD \quad (5.a)$
Rain rate R_T $[mm \cdot h^{-1}]$ (3.67)	$R_T = \frac{6\pi}{10^4} \sum_i D_i^3 V(D_i) N(D_i) \Delta D_i \quad (6.a)$
The liquid water content W $[g \cdot m^{-3}]$ (3)	$W = \frac{\pi}{6 \cdot 10^3} \sum_i D_i^3 N(D_i) \Delta D_i \quad (7.a)$
Radar reflectivity (Rayleigh approximation) Z $[mm^6 \cdot m^{-3}]$ (6)	$Z = \sum_i D_i^6 N(D_i) \Delta D_i \quad (8.a)$
The drop energy flux (rate of kinetic energy) E $[J \cdot m^{-2} \cdot h^{-1}]$ (5.01)	$E = \frac{3\pi}{10^4} \sum_i D_i^3 [Vt(D_i)]^3 N(D_i) \Delta D_i \quad (9.a)$

Table 1.b. Expressions of meteorological variables formulated with the DSD using R (D) function (more details in [15]).

Name of variables (Order of m_n)	Formula
The measured moment of the DSD (n)	$m_n = \sum_i D_i^n R(D_i) \Delta D_i \quad (4.b)$
The theoretical moment of the DSD (n)	$m_n = \int_0^{+\infty} D^n R(D) dD \quad (5.b)$
Rain rate R_T $[mm \cdot h^{-1}]$ (0)	$R_T = \sum_i R(D_i) \Delta D_i \quad (6.b)$
The liquid water content W $[g \cdot m^{-3}]$ (-0.67)	$W = \frac{10}{36} \sum_i \frac{R(D_i)}{V(D_i)} \Delta D_i \quad (7.b)$
Radar reflectivity (Rayleigh approximation) Z $[mm^6 \cdot m^{-3}]$ (2.33)	$Z = \frac{10^4}{6\pi} \sum_i \frac{D_i^3 R(D_i)}{V(D_i)} \Delta D_i \quad (8.b)$
The drop energy flux (rate of kinetic energy) E $[J \cdot m^{-2} \cdot h^{-1}]$ (1.34)	$E = \frac{1}{2} \sum_i [Vt(D_i)]^2 R(D_i) \Delta D_i \quad (9.b)$

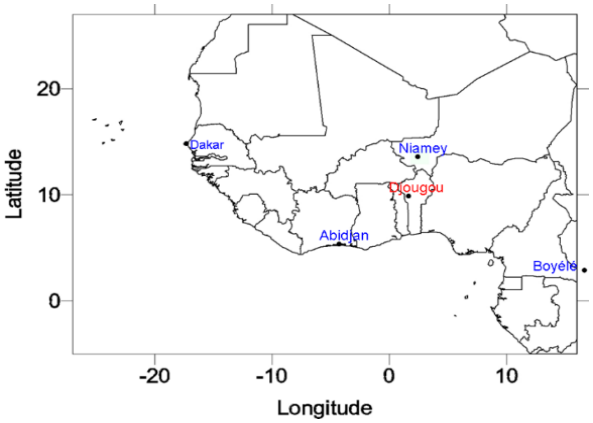

Fig. 1. West Africa region with the cities in which the DSD was sampled once. The DSDs used in this study were sampled around the city of Djougou.

II. DATA

Optical disdrometers belong to the new generation of sensors that measure the size of raindrops ([20]-[22]). There are currently two types: Optical disdrometers with only one beam (OSP: Optical Spectro-Pluviometer) and those with double beam (DBS: Dual Beam Spectro-pluviometer). During the Enhanced Observing Period (EOP) of the AMMA campaign ([23] or web site http://www.amma-international.org), these two types of optical disdrometers have been used to reinforce the observations of weather radar installed in Djougou northern of Benin (Fig.1). For technical reasons, these instruments did not work simultaneously. The characteristics of the instruments, the geographical coordinates of their installation points and the operating periods are presented in Table 2. During three rainy seasons (2005 to 2007), these optical disdrometers observed the rain on three sites, in the center and around the city of Djougou (Fig.1). Overall, 93 events have been sampled, which represent 11647 spectra of DSD (of duration one minute) and 1221 mm of cumulated rain. The comparison ([24]) of these measures to those of rain gauges located near the disdrometers showed a good similarity both in terms of the event accumulations and intensity distributions.

In this study, all the analysis that will be performed will depend on these data. For the relevance of the analysis, this disdrometric database has been divided into two samples:

- DATA A consists of 47 events, a total of 6175 spectra of DSD, used for the modeling of the distribution;
- DATA B consists of 46 events, a total of 5472 spectra of DSD, used for the validation of the moments' model.

From our data, we calculated respectively, for each spectrum, the $N(D)$ and $R(D)$ functions with the formulas (1) and (3). We then calculated the measured moments of order n of each function.

Table 2. Synthesis of the disdrometers data measured in northern Benin: characteristics of the used disdrometers; coordinates of the measuring sites; and operating periods of each sensor. IR: Infrared (Source: [12]).

Sensor name / Type of disdrometer / Horizontal section	Location / Coordinates	operating period	Number of events/ Number of spectra / Total cumulative rainfall
Parsivel / OSP with one beam IR / $S = 48.6cm^2$	Nangatchiori / 1.74° E, 9.65° N	August to October 2005	10 events / 1816 spectra / 160.03 mm
DBS-01 / OSP double beam IR / $S = 100cm^2$	Copargo / 1.56° E, 9.82° N	June to September 2006	27 events / 3101 spectra / 325.12 mm
OSP-01 / OSP double beam IR / $S = 100cm^2$	Djougou / 1.66°E, 9.69°N	June to September 2006	14 events / 1772 spectra / 256.10mm
OSP-02 / OSP with one beam IR / $S = 100cm^2$	Djougou / 1.66°E, 9.69°N	June to October 2007	42 events / 4958 spectra / 479.65mm

International Journal of Research and Innovations in Earth Science
Volume 5, Issue 6, ISSN (Online): 2394-1375

III. METHOD

Several authors such as [6] and [7] showed that the parameters of the individual spectra are generally strongly dispersed. This has led other authors ([15]-[18]; and [25]) to calculate and analyze the average of the DSD by rain rate class. This same situation has led other authors such as: [5] to suggest a normalization of the DSD with a single parameter; [26] or [27] to suggest a normalization of the DSD with two parameters.

In this work, we adopted the method used by [15]-[18]; and [25]. Successively, we have:

- Grouped the measured spectra of DATA A by rainfall rate classes;
- Calculated the average of the distributions of each class, and for each function ($N(D)$ and $R(D)$);
- Calculated the moments of order n of each average distribution;
- Modeled these average distributions by gamma law or lognormal law using the relationships established in Table 3.a and 3.b;
- Established the relationship between the model parameters and the rainfall rate;
- Compared the estimated moments with the measured moments using the measurements of DATA B.

Table 3.a. Expression of the gamma and lognormal laws and their adjustments by the method of moments (case of the $N(D)$ function).

Gamma law		
Expression of the law	$N(D) = \frac{N_T(\mu+1)^{(\mu+1)}}{D_c\Gamma(\mu+1)}\left(\frac{D}{D_c}\right)^{\mu} exp\left[-(\mu+1)\frac{D}{D_c}\right]$	(10.a)
Theoretical moment of order n	$M_n = \frac{N_T}{\Gamma(\mu+1)}\left(\frac{D_c}{\mu+1}\right)^{n}\Gamma(\mu+n+1)$	(11.a)
Total number of drops $[m^{-3}]$	$N_T = M_0$	(12.a)
Characteristic diameter $[mm]$	$D_c = \frac{M_1}{M_0}$	(13.a)
Shape parameter	$\mu = \frac{M_0M_2 - 2M_1^2}{M_1^2 - M_0M_2}$	(14.a)
Lognormal law		
Expression of the law	$N(D) = \frac{N_T}{\sqrt{2\pi}Dln\sigma} exp\left[-\frac{ln^2(D/D_g)}{2ln^2\sigma}\right]$	(10.b)
Theoretical moment of order n	$M_n = N_T D_g^n exp\left(\frac{1}{2}n^2ln^2\sigma\right)$	(11.b)
Total number of drops $[m^{-3}]$	$N_T = M_0$	(12.b)
Characteristic diameter $[mm]$	$D_g = \frac{M_1}{M_0}\sqrt{\frac{M_1^2}{M_0M_2}}$	(13.b)
Shape parameter	$\sigma = exp\left[\sqrt{-ln\left(\frac{M_1^2}{M_0M_2}\right)}\right]$	(14.b)
Relationship between the two laws		
Characteristic diameters and Shape parameters	$\left(\frac{D_g}{D_c}\right)^2 = \frac{\mu+1}{\mu+2}$	(15.a)
	$\left(\frac{D_g}{D_c}\right)^2 = exp(-ln^2\sigma)$	(15.b)
Shape parameters of the two laws	$ln^2\sigma = ln\left(\frac{\mu+2}{\mu+1}\right)$	(15.c)

IV. RESULTS AND ANALYSIS

The sample DATA A is used for modeling. Fig.2 (respectively 3) describes the average distributions and their modelizations with the gamma and lognormal laws, for the $N(D)$ (respectively $R(D)$) function. The values of the model parameters adjusted to the average distributions are presented in Table 4.a and 4.b. The correlation and Nash coefficients are calculated between the average distributions and the models. These coefficients are entered in these same Tables. Fig.4 (respectively 5) describes the trend of the model parameters according to the rainfall rate, for the $N(D)$ (respectively $R(D)$) function. The relationships established between these parameters and the rainfall rate are presented in Table 5. It can therefore be seen that the DSDs measured in northern Benin, with both the $N(D)$ function and the $R(D)$ function, are well modeled by the gamma law or the lognormal law.

Table 3.b. Expression of the gamma and lognormal laws and their adjustments by the method of moments (case of the $R(D)$ function)

Gamma law		
Expression of the law	$R(D) = \frac{R_T(\mu'+1)^{(\mu'+1)}}{D_c'\Gamma(\mu'+1)}\left(\frac{D}{D_c'}\right)^{\mu'} exp\left[-(\mu'+1)\frac{D}{D_c'}\right]$	(16.a)
Theoretical moment of order n	$m_n = \frac{R_T}{\Gamma(\mu'+1)}\left(\frac{D_c'}{\mu'+1}\right)^{n}\Gamma(\mu'+n+1)$	(17.a)
Rainfall rate $[mm\cdot h^{-1}]$	$R_T = m_0$	(18.a)
Characteristic diameter $[mm]$	$D_c' = \frac{m_1}{m_0}$	(19.a)
Shape parameter	$\mu' = \frac{m_0m_2 - 2m_1^2}{m_1^2 - m_0m_2}$	(20.a)
Lognormal law		
Expression of the law	$R(D) = \frac{R_T}{\sqrt{2\pi}Dln\sigma'} exp\left[-\frac{ln^2(D/D_g')}{2ln^2\sigma'}\right]$	(16.b)
Theoretical moment of order n	$m_n = R_T {D_g'}^n exp\left(\frac{1}{2}n^2ln^2\sigma'\right)$	(17.b)
Rainfall rate $[mm\cdot h^{-1}]$	$R_T = m_0$	(18.b)
Characteristic diameter $[mm]$	$D_g' = \frac{m_1}{m_0}\sqrt{\frac{m_1^2}{m_0m_2}}$	(19.b)
Shape parameter	$\sigma' = exp\left[\sqrt{-ln\left(\frac{m_1^2}{m_0m_2}\right)}\right]$	(20.b)
Relationship between the two laws		
Characteristic diameters and Shape parameters	$\left(\frac{D_g'}{D_c'}\right)^2 = \frac{\mu'+1}{\mu'+2}$	(21.a)
	$\left(\frac{D_g'}{D_c'}\right)^2 = exp(-ln^2\sigma')$	(21.b)
Shape parameters of the two laws	$ln^2\sigma' = ln\left(\frac{\mu'+2}{\mu'+1}\right)$	(21.c)

International Journal of Research and Innovations in Earth Science
Volume 5, Issue 6, ISSN (Online): 2394-1375

A. *Analysis of the Trend of Model Parameters According to the Rainfall Rate*

The total number of drops per unit volume (N_T), and the diameters characteristic of the average size of the drops (D_c and D_g) increase according to the rainfall rate (R_T). Obviously, the increase in the rainfall rate is justified by the joint increase of the number of drops and the size of the drops. The relations obtained are in agreement with those established by other authors: [17]-[18] in West Africa; and [25] in Brazil.

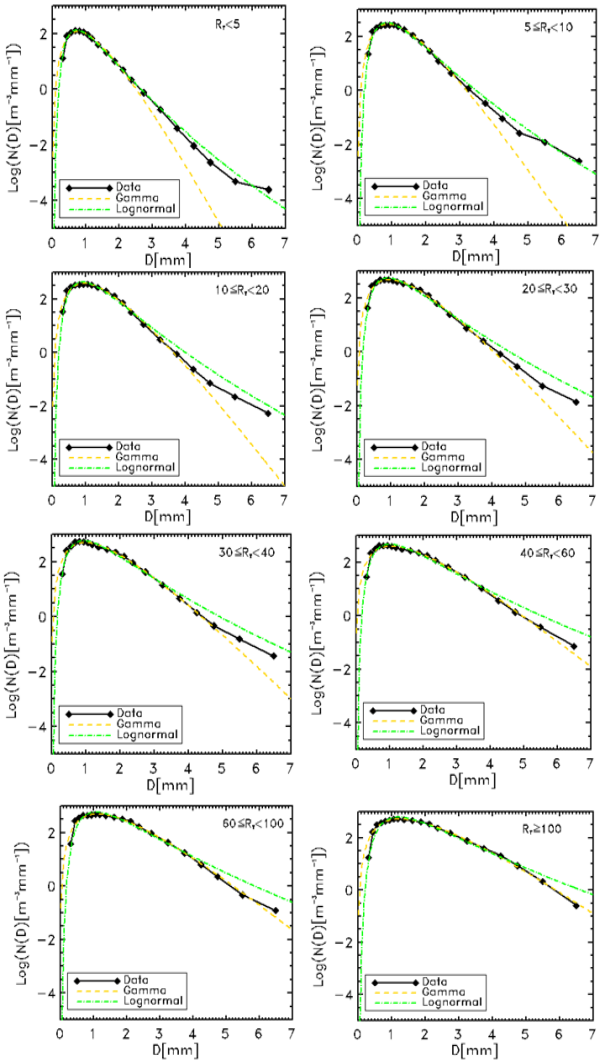

Fig. 2. Sample DATA A, $N(D)$ function: the average DSDs of the eight rain rate classes are represented by the symbol; and the curves adjusted on these average DSDs are represented by lines.

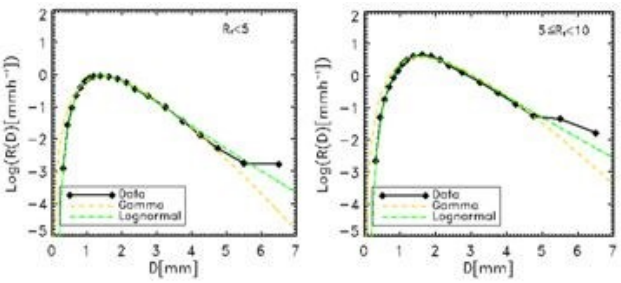

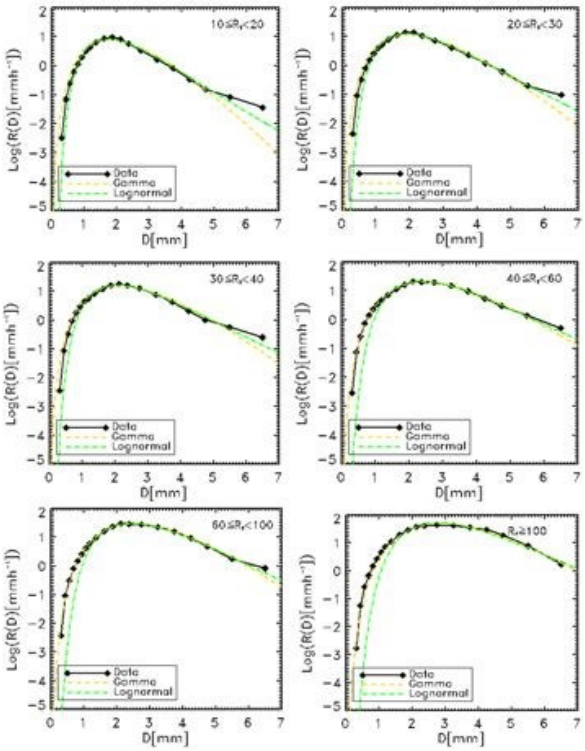

Fig. 3. Sample DATA A, $R(D)$ function: the average DSDs of the eight rain rate classes are represented by the symbol; and the curves adjusted on these average DSDs are represented by lines.

In Table 3.a and 3.b, we have established a relationship between the shape parameters of the gamma and lognormal laws: μ and σ for the $N(D)$ function on the one hand; and μ' and σ' for the $R(D)$ function on the other hand. Fig.6 shows that there is a very good agreement between this relationship and the adjusted values of these parameters. We analyze the trend of shape parameters for each function:

Case of the function $N(D)$: From our data, the shape parameter μ of the gamma law decreases according to R_T. Thus, the slope parameter $\Lambda = \frac{\mu+1}{D_c}$ also decreases according to R_T (since D_c increases according to R_T). This is in agreement with the results of several authors such as [13], [3], [28], etc. Furthermore, several other authors ([10]; [29] and [30]) have shown that the shape parameter μ increases with the slope parameter Λ. So if the shape parameter μ decreases according to R_T, it is normal for the slope parameter Λ to decrease according to R_T. Nevertheless, it should be noted that this result is at odds with that obtained by [17] who found that μ and Λ increase according to the rainfall rate. Moreover, since μ decreases according to R_T, it is completely obvious (referring to Fig.6) that the shape parameter σ of the lognormal law increases according to R_T. It is this result that we obtained in this article, in agreement with that of [25], but in disagreement with those of [4], [17], and [18].

Case of the function R (D): From our data, the shape parameter μ' of the gamma law increases according to R_T and the shape parameter σ' of the lognormal law decreases according to R_T. With respect to R_T, the trend of μ' (respectively σ') is the inverse of that μ (respectively σ). In

the expression (3) of the $R(D)$ function, we note the absence of the term of the falling drop velocity compared to the expression (1) of the $N(D)$ function. This would certainly be the cause of the inversion of the trend of shape parameters, between the $N(D)$ function and the $R(D)$ function.

B. *Comparison of Estimated Moments and Measured Moments*

Sample DATA B is used for the validation of the modeling. We made a comparison (spectra to spectra) of measured moments and estimated moments, using the criteria defined in the appendix. To calculate the estimated moments of the $N(D)$ function, we used the formulas (11.a and 11.b) in Table 3.a and the relationships (22a), (23a), (24a), (22b), (23b), (24b) in Table 5. To calculate the estimated moments of the $R(D)$ function, we used the formulas (17.a and 17.b) in Table 3.b and the relationships (25a), (26a), (25b) and (26b) in Table 5. Table 1.a and 1.b indicates that the useful moments belong to the range: $[3, 6]$ for the $N(D)$ function; and $[-0.67, 2.33]$ for the $R(D)$ function. Fig.7 (respectively 8) describes the four comparison criteria for the function $N(D)$ (respectively $R(D)$). For the $N(D)$ function, the gamma law estimates the moments of order between 5 and 6 better than the lognormal law. For the $R(D)$ function, the lognormal law estimates the moments of order between -2 and -1 better than the gamma law. It is therefore not possible to discriminate between these two laws. Comparing the functions, we see that the $R(D)$ function estimates these useful moments better than the $N(D)$ function. This result is probably due to the fact that for the $N(D)$ function three parameters were adjusted according to the rainfall rate, whereas for the $R(D)$ function it was necessary to adjust only two parameters as a function of the rate rain. Fig.9 shows the comparison between measured and estimated radar reflectivity (with each function), and confirms the above result.

Table 4.a. Values of model parameters adjusted to the average distributions of each rainfall rate class. The coefficients ρ (of correlation) and Nash are calculated between the average distribution and the adjusted model (case of the $N(D)$ function).

Rain rate classes	$R_T <$ 5	$5 \leq R_T < 10$	$10 \leq R_T < 20$	$20 \leq R_T < 30$
Number of spectra	4589	573	428	228
Mean of $R_T[mm \cdot h^{-1}]$	1.442	6.972	14.300	24.300
Parameters	**Gamma law**			
$N_T[m^{-3}]$	110.86	309.412	466.998	630.984
$D_c\ [mm]$	0.936	1.099	1.187	1.229
μ	4.242	4.316	3.977	3.382
ρ	0.991	0.994	0.991	0.988
$Nash$	0.978	0.987	0.981	0.976
Parameters	**Lognormal law**			
$N_T[m^{-3}]$	110.86	309.412	466.998	630.984
$D_g\ [mm]$	0.858	1.009	1.083	1.109
σ	1.519	1.515	1.534	1.574
ρ	0.996	0.982	0.975	0.978
$Nash$	0.992	0.954	0.930	0.941
Rain rate classes	$30 \leq R_T < 40$	$40 \leq R_T < 60$	$60 \leq R_T < 100$	$R_T \geq 100$
Number of spectra	124	122	78	33
Mean of $R_T[mm \cdot h^{-1}]$	34.370	48.691	72.232	132.223
Parameters	**Gamma law**			
$N_T[m^{-3}]$	711.805	650.429	846.122	994.029
$D_c\ [mm]$	1.285	1.422	1.493	1.679
μ	3.084	2.703	2.873	2.886
ρ	0.985	0.980	0.985	0.994
$Nash$	0.966	0.957	0.969	0.986
Parameters	**Lognormal law**			
$N_T[m^{-3}]$	711.805	650.429	846.122	994.029
$D_g\ [mm]$	1.151	1.262	1.331	1.498
σ	1.597	1.631	1.615	1.614
ρ	0.986	0.970	0.958	0.976
$Nash$	0.967	0.924	0.881	0.932

Table 4.b. Values of model parameters adjusted to the average distributions of each rainfall rate class. The coefficients ρ (of correlation) and Nash are calculated between the average distribution and the adjusted model (case of the $R(D)$ function).

Rain rate classes	$R_T < 5$	$5 \leq R_T < 10$	$10 \leq R_T < 20$	$20 \leq R_T < 30$
Parameters	**Gamma law**			
$R_T[mm \cdot h^{-1}]$	1.442	6.957	14.263	24.249
$D_c'\ [mm]$	1.740	1.949	2.092	2.310
μ'	4.796	4.908	5.837	5.610
ρ	0.993	0.976	0.980	0.984
$Nash$	0.978	0.933	0.949	0.957
Parameters	**Lognormal law**			
$R_T[mm \cdot h^{-1}]$	1.442	6.957	14.263	24.249
$D_g'\ [mm]$	1.607	1.803	1.954	2.153
σ'	1.490	1.485	1.447	1.455
ρ	0.999	0.991	0.988	0.991
$Nash$	0.997	0.980	0.976	0.982
Rain rate classes	$30 \leq R_T < 40$	$40 \leq R_T < 60$	$60 \leq R_T < 100$	$R_T \geq 100$
Parameters	**Gamma law**			
$R_T[mm \cdot h^{-1}]$	34.246	48.507	71.999	131.395
$D_c'\ [mm]$	2.505	2.836	2.884	3.268
μ'	5.622	6.273	6.623	7.239
ρ	0.989	0.997	0.997	0.994
$Nash$	0.971	0.993	0.99	0.985
Parameters	**Lognormal law**			
$R_T[mm \cdot h^{-1}]$	34.246	48.507	71.999	131.395
$D_g'\ [mm]$	2.335	2.659	2.712	3.086
σ'	1.455	1.432	1.421	1.403
ρ	0.991	0.995	0.995	0.983
$Nash$	0.982	0.985	0.984	0.944

International Journal of Research and Innovations in Earth Science
Volume 5, Issue 6, ISSN (Online): 2394-1375

Table 5. Relationships established between model parameters and the rainfall rate. The coefficients ρ (of correlation) and *Nash* are calculated between the parameter and the adjusted relation.

Relationship		ρ	*Nash*
$N(D)$ Function – Gamma law			
$N_T = 112.86R_T^{0.465}$	$(22.a)$	0.965	0.907
$D_c = 0.862R_T^{0.126}$	$(23.a)$	0.980	0.957
$\mu = 4.834R_T^{-0.116}$	$(24.a)$	0.872	0.758
$N(D)$ Function – Lognormal law			
$N_T = 112.86R_T^{0.465}$	$(22.b)$	0.965	0.907
$D_g = 0.798R_T^{0.118}$	$(23.b)$	0.976	0.951
$\sigma = 1.488R_T^{0.018}$	$(24.b)$	0.882	0.778
$R(D)$ Function – Gamma law			
$D_c' = 1.459R_T^{0.160}$	$(25.a)$	0.973	0.947
$\mu' = 4.283R_T^{0.098}$	$(26.a)$	0.926	0.857
$R(D)$ Function – Lognormal law			
$D_g' = 1.406R_T^{0.151}$	$(25.b)$	0.973	0.942
$\sigma' = 1.509R_T^{-0.013}$	$(26.b)$	0.926	0.857

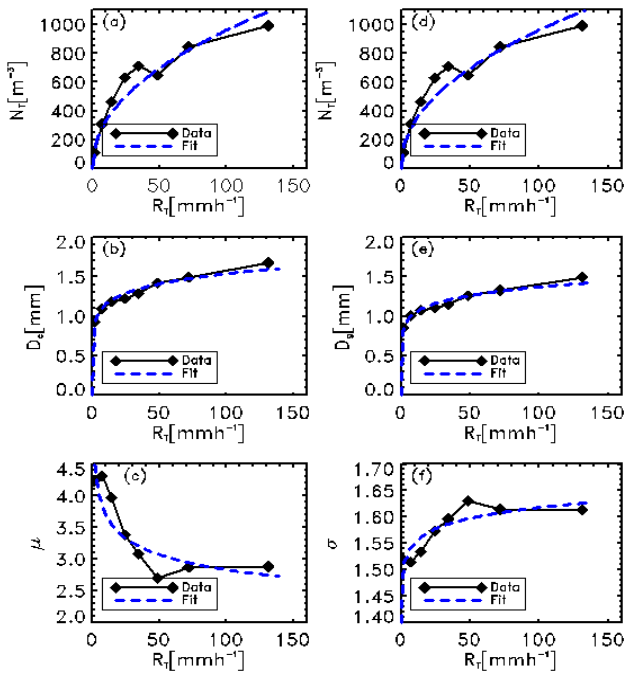

Fig. 4. Sample DATA A, $N(D)$ function, trend of the parameters of the models according to the rate of rain: (a), (b) and (c) respectively represent the parameters N_T, D_c and μ of the gamma law; (d), (e) and (f) respectively represent the parameters N_T, D_g and σ of the lognormal law. NB: (a) and (d) are identical.

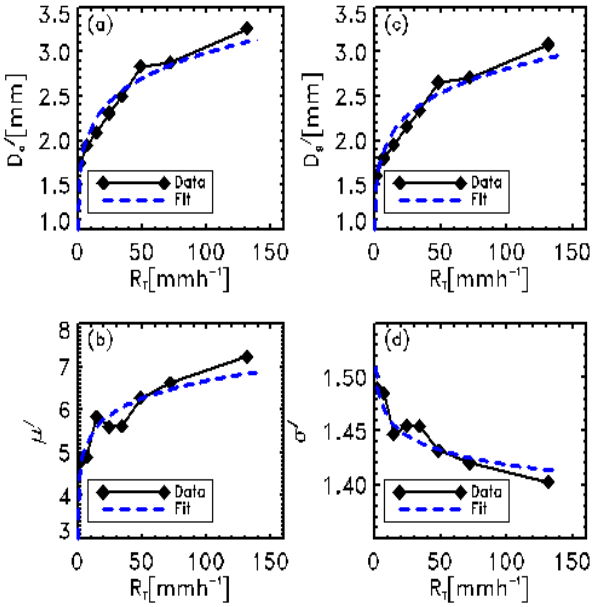

Fig. 5. Sample DATA A, $R(D)$ function, trend of the parameters of the models according to the rate of rain: (a) and (b) respectively represent the parameters D_c' and μ' of the gamma law; (c) and (d) respectively represent the parameters D_g' and σ' of the lognormal law.

V. Conclusion

Usually, the DSD is analyzed with the $N(D)$ function which is equal to the number of raindrops per unit of volume and per diameter range. Recently, [15] analyzed it with the $R(D)$ function which is equal to the rainfall rate per interval of diameters. All meteorological variables that are formulated using the $N(D)$ function can also be formulated using the $R(D)$ function (see Table 1).

In this paper, the DSDs measured in northern Benin (West Africa) are analyzed with the $N(D)$ and $R(D)$ functions. Eight classes of rain rates are created and the average DSDs in these classes are modeled with the gamma and lognormal laws. Relationships are established between the parameters of these models and the rainfall rate. These DSDs are thus parameterized with the rainfall rate. The efficiency of this parameterization was evaluated by comparing the estimated useful moments and the measured useful moments. From this evaluation, it appears that the $R(D)$ function estimates its useful moments better than the function $N(D)$. Moreover, we have shown that there is no significant difference between DSD modeling by the gamma law and DSD modeling by the lognormal law. In addition, we have established a relationship between the shape parameters of these two laws. This relation thus makes it possible to pass from the gamma law to the lognormal law and reciprocally.

International Journal of Research and Innovations in Earth Science
Volume 5, Issue 6, ISSN (Online): 2394-1375

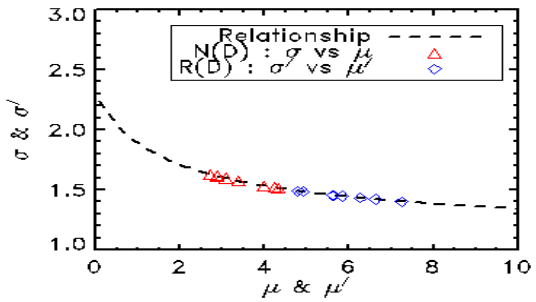

Fig. 6. Relationship between the shape parameters of the gamma (μ or μ′) and lognormal (σ or σ′) laws. The established relationship is presented by line. The symbols are the values of the shape parameters adjusted on the average DSDs.

APPENDIX

Let Y^{obs} be an observed data or directly calculated from the observations, and Y^{est} be a theoretically estimated data, $E[Y^{obs}]$ and $E[Y^{est}]$ their respectively averages, and σ_{obs} and σ_{est} their respectively standard deviations, the four criteria used to test the efficacy of the model suggested are defined as follows:

- The coefficient of linear correlation of Pearson: $\rho = \frac{E[(Y^{obs}-E[Y^{obs}])(Y^{est}-E[Y^{est}])]}{\sigma_{obs}\sigma_{est}}$
- The mean relative error : $< RE > = E\left[\frac{(Y^{est}-Y^{obs})}{Y^{obs}}\right]$
- The Nash coefficient [31], defined by:

$$Nash = 1 - \frac{E[(Y^{est} - Y^{obs})^2]}{E[(Y^{obs} - E[Y^{obs}])^2]}$$

- The efficiency coefficient KGE of [32], defined by:

$$KGE = 1 - \sqrt{(\rho - 1)^2 + (\frac{\sigma_{est}}{\sigma_{obs}} - 1)^2 + (\frac{E[Y^{est}]}{E[Y^{obs}]} - 1)^2}.$$

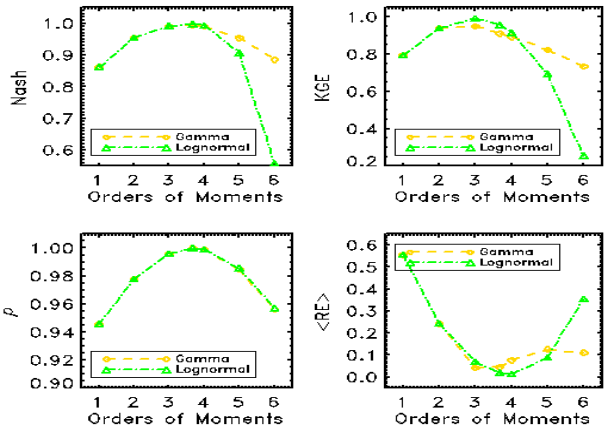

Fig. 7. Sample DATA B, $N(D)$ function, validation of the modeling: comparison (spectrum to spectrum) of measured moments and estimated moments. Successively: the $Nash$ coefficient; the coefficient KGE; the linear correlation coefficient ρ; and the mean relative error $< RE >$.

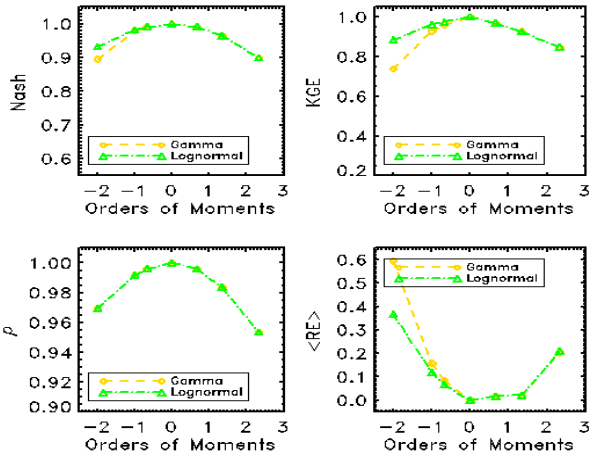

Fig. 8. Sample DATA B, $R(D)$ function, validation of the modeling: comparison (spectrum to spectrum) of measured moments and estimated moments. Successively: the $Nash$ coefficient; the coefficient KGE; the linear correlation coefficient ρ; and the mean relative error $< RE >$.

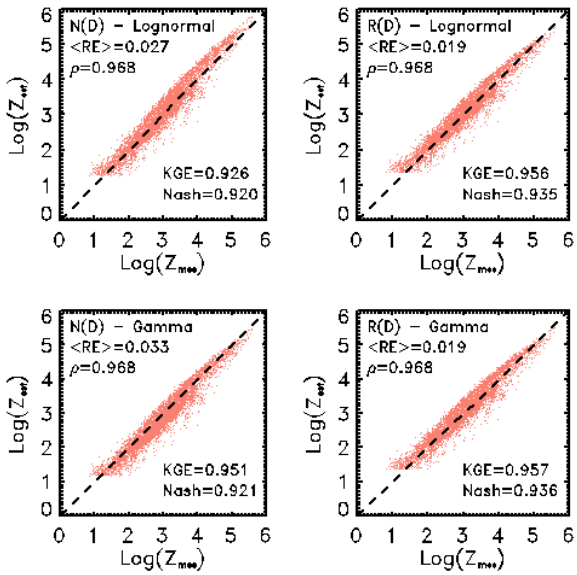

Fig. 9. Sample DATA B, radar reflectivity Z (estimated according to measured): the line represents the first bisector; on the left the estimate is made with the $N(D)$ function (lognormal and gamma); on the right the estimate is made with the $R(D)$ function (lognormal and gamma).

ACKNOWLEDGMENT

Based on a French initiative, AMMA was built by an international scientific group and is currently funded by a large number of agencies, especially from France, UK, US and Africa. It has been the beneficiary of a major financial contribution from the European Community's Sixth Framework Research Program. Detailed information on scientific coordination and funding is available on the AMMA International web site http://www.amma-international.org .

REFERENCES

[1] Waldvogel A., "The N0 jump of raindrop spectra," J. Atmos. Sci., vol. 31, 1974, pp. 1067-1078.

[2] Ulbrich, C. W., "Natural variation in the analytical form of the raindrop size distribution," J. Climate Appl. Moteor., vol. 22, 1983, pp. 1764-1775.

[3] Willis P. T., "Functional fits to some observed drop size distributions and paramétrisation of rain," J. Atmos. Sci., vol. 41, 1984, pp. 1648-1661.

[4] Feingold G., Levin Z., "The lognormal fit of raindrop spectra from frontal convective clouds in Israel," J. Clim. Appl. Meteor., vol. 25, 1986, pp. 1346-1363.

[5] Sempere-Torres D., Porra J. M., Creutin J. D., "A general formulation for raindrop size distribution.," J. Appl. Meteorol., vol. 33, 1994, pp. 1494-1502.

[6] Tokay A., Short D. A., "Evidence from tropical raindrop spectra of the origin of rain from stratiform versus convective Clouds," J. Appl. Meteor., vol. 35, 1996, pp. 355-371.

[7] Maki M., Keenan T. D., Sasaki Y., Nakamura K., "Characteristics of the raindrop size distribution in tropical continental squall lines observed in Darwin, Australia," J. Appl. Meteor., vol. 40, 2001, pp. 1393-1412.

[8] Bringi V. N., Huang G-J., Chandrasekar V., "A Methodology for estimating the parameters of a gamma raindrop size distribution model from polarimetric radar data: application to a squall-line event from the TRMM/Brazil campaign," J. Atmos. Ocean. Techn., vol. 19, 2002, pp. 633-645.

[9] Uijlenhoet R., Steiner M., Smith J. A., "Variability of raindrop size distributions in a squall line and implication for radar rainfall estimation," J. Hydrometeor., vol. 4, 2003, pp. 43-61.

[10] Vivekanandan J., Zhang G., Brandes E., "Polarimetric radar estimators dased on a constrained gamma drop Size distribution model," J. Appl. Meteor., vol. 43, 2004, pp. 217-230.

[11] Lee G. W., Zawadzki I., "Variability of drop size distributions: time-scale dependence of the variability and its effects on rain estimation," J. Appl. Meteor., vol. 44, 2005, pp. 241-255.

[12] Moumouni S., Gosset M., Houngninou E., "Main features of rain drop size distributions observed in Benin, West Africa, with optical disdromètres," Geophys. Res. Lett., vol. 35, 2008, L23807 DOI: 10.1029/2008GL035755.

[13] Marshall J.S., Palmer W. Mc. K., "The distribution of raindrop with size," J. Meteor., vol. 5, 1948, pp. 165-166.

[14] Atlas D., Ulbrich C. W., "Path and area-integrated rainfall measurement by microwave attenuation in the 1-3 cm band," J. App. Meteor., vol. 16, 1977, pp. 1322-1331.

[15] Kougbéagbédè H., Houngninou B. E., Moumouni S. "Modeling rain rate distribution per diameter class from disdrometer data collected in northern Benin (AMMA Campaign): a new relationship between radar reflectivity and rainfall rate," IJRIES, vol. 4(3), 2017, pp. 2394-1375.

[16] Sauvageot H., Lacaux J. P., "The shape of averaged drop size distributions," J. Atmos. Sci., vol. 52, 1995, pp. 1070-1083.

[17] Nzeukou A., Sauvageot H., Ochou A. D., Kebe C. M. F., "Raindrop size distribution and radar parameters at Cape Verde," J. Appl. Meteor., vol. 43, 2004, pp. 90-105.

[18] Ochou A. D., Nzeukou A., Sauvageot H., "Parameterization of drop size distribution with rain rate," Atmos. Res., vol. 84, 2007, pp. 58-66.

[19] Ochou A. D., "Variabilité spatio-temporelle des moments statistiques des distributions des gouttes de pluie et conséquences sur la mesure des précipitations par télédétection micro-ondes," Thèse d'état Université Cocody-Abidjan, 2003.

[20] Salles C., Creutin J. D., Sempere-Torres D., "The optical spectropluviometer revisited," J. Atmos. Oceanic. Technol., vol. 15, 1998, pp. 1215-1222.

[21] Löffler-Mang M., Joss J., "An optical disdrometer for measuring size and velocity of hydrometeors," J. Atmos. Oceanic. Technol., vol. 17, 2000, pp. 130-139.

[22] Delahaye J-Y., Barthès L., Golé P., Lavergnat J., Vinson J. P., "A dual-beam spectropluviometer concept," J. of Hydrology, vol. 328, 2005, pp. 110-120.

[23] Redelsperger J-L., Thorncroft C., Diedhiou A., Lebel T., Parker D., Polcher J., "African Monsoon, Multidisciplinary Analysis (AMMA): An International Research Project and Field Campaign," Bull. Amer. Meteor. Soc., vol. 88, 2006, pp. 1739-1746.

[24] Moumouni S., "Analyse des distributions granulométriques des pluies au Bénin : caractéristiques globales, variabilité et application à la mesure radar," Thèse de Doctorat INP-Grenoble, 2009.

[25] Tenorio R. S., da Silva Moraes M. C., Sauvageot H., "Raindrop size distribution and radar parameters in Coastal Tropical Rain Systems of Northeastern Brazil," J. Appl. Meteor. Clim., vol. 51, 2012, pp. 196-1970.

[26] Testud J., Oury S., Black R. A., Amayenc P., Dou X., "The concept of ''normalized'' distribution to describe raindrop spectra: A tool for cloud physics and cloud remote sensing," J. Appl. Meteorol., vol. 40, 2001, pp. 1118-1140.

[27] Lee G. W., Zawadzki I., Szyrmer W., Sempere-Torres D., Uijlenhoet R., "A general approach to double-moment normalization of drop size distributions," J. Appl. Meteor., vol. 43, 2004, pp. 264-281.

[28] Cerro C., Codina B., Bech J., Lorente J., "Modeling raindrop size distribution and Z(R) relations in the western Mediterranean area," J. Appl. Meteor., vol. 36, 1997, pp. 1470-1479.

[29] Brandes E. A., Zhang G., Vivekanandan J., "An evaluation of a drop distribution–dased polarimetric radar rainfall estimator," J. Appl. Meteor., vol. 42, 2003, pp. 652-660.

[30] Zhang G., Vivekanandan J., Brandes E. A., Meneghini R., Kozu T., "The shape-slope relation in observed gamma raindrop size distributions: Statistical error or useful information?," J. Atmos. Oceanic Technol., vol. 20, 2003, pp. 1106–1119.

[31] Nash J. E., Sutcliffe J. V., "River flow forecasting through conceptual models part I - A discussion of principles," J. Hydrol., vol. 10, 1970, pp. 282-290.

[32] Gupta H. V., Kling H., Yilmaz K. K., Martinez G. F., "Decomposition of the mean squared error and NSE performance criteria: Implications for improving hydrological modeling," J. Hydrol., vol. 377, 2009, pp. 80-91, DOI:10.1016/ j.jhydrol.2009.08.003.

AUTHORS PROFILE'

Dr Sounmaïla MOUMOUNI
Is a Senior Lecturer in Higher Teachers' Training School of Natitingou, University of Parakou, Republic of Benin (West Africa). Research interest: (1) Meteorological process and Climate Change; (2) Theoretical study of diffusion process and its applications. E-mail: sounma.moumouni@gmail.com

Mr Loic Saturnin ADJIKPE
Is a PhD student at the Faculty of Sciences and Technology of the University of Abomey-Calavi, Republic of Benin (West Africa). Research interest: Meteorological process and Climate Change. E-mail: alosatur@gmail.com

Dr Siaka MASSOU
Is a Senior Lecturer in Department of Physics of the Faculty of Sciences and Technology of the University of Abomey-Calavi, Republic of Benin (West Africa). Research interest: (1) Stochastics process and its applications; (2) Theoretical study of diffusion process and its applications. E-mail: siakmas@yahoo.fr

Dr Agnidé Emmanuel LAWIN
Is a Senior Lecturer in Laboratory of Applied Hydrology of the National Water Institute of the University of Abomey-Calavi, Republic of Benin (West Africa). Research interest: (1) Meteorological process and Climate Change; (2) Hydrology. E-mail: ewaari@yahoo.fr